Branched versus Linear Structure: Lowering the CO$_2$ Desorption Temperature of Polyethylenimine-Functionalized Silica Adsorbents

Jannis Hack, Seraina Frazzetto, Leon Evers, Nobutaka Maeda * and Daniel M. Meier *

Institute of Materials and Process Engineering (IMPE), School of Engineering (SoE), Zurich University of Applied Sciences (ZHAW), CH-8400 Winterthur, Switzerland; hacj@zhaw.ch (J.H.); serainafrazzetto@outlook.com (S.F.); ever@zhaw.ch (L.E.)
* Correspondence: maeo@zhaw.ch (N.M.); meid@zhaw.ch (D.M.M.)

Abstract: Lowering the regeneration temperature for solid CO$_2$-capture materials is one of the critical tasks for economizing CO$_2$-capturing processes. Based on reported pKa values and nucleophilicity, we compared two different polyethylenimines (PEIs): branched PEI (BPEI) and linear PEI (LPEI). LPEI outperformed BPEI in terms of adsorption and desorption properties. Because LPEI is a solid below 73–75 °C, even a high loading amount of LPEI can effectively adsorb CO$_2$ without diffusive barriers. Temperature-programmed desorption (TPD) demonstrated that the desorption peak top dropped to 50.8 °C for LPEI, compared to 78.0 °C for BPEI. We also revisited the classical adsorption model of CO$_2$ on secondary amines by using in situ modulation excitation IR spectroscopy, and proposed a new adsorption configuration, R1(R2)-NCOOH. Even though LPEI is more expensive than BPEI, considering the long-term operation of a CO$_2$-capturing system, the low regeneration temperature makes LPEI attractive for industrial applications.

1. Introduction

A record-high level of CO$_2$ concentration in the atmosphere (ca. 415 ppm) poses a global concern about how to suppress or stop anthropogenic CO$_2$ emissions [1]. CO$_2$ capture technology is considered to help to reduce the CO$_2$ concentration in the atmosphere. It falls into two categories: direct CO$_2$ capture from the air (ca. 415 ppm CO$_2$) [2] and CO$_2$ capture from power plants and other industrial sectors (4–100% CO$_2$) [3,4]. In either case, the regeneration temperature to collect the adsorbed CO$_2$ is as high as 80–120 °C. With regard to adsorbent degradation and operation cost, lowering the regeneration temperature is strongly desired [5,6]. Traditionally, liquid amine scrubbing has been employed for CO$_2$ capture [5,7]. However, its downsides, such as loss of volatile amine, corrosion, and high energy consumption in the regeneration step, make industries long for an alternative capturing system [8]. In this regard, solid adsorbents such as mesoporous oxides, zeolites, and metal–organic frameworks (MOFs) have recently gained attention due to their feasibility for desorbing CO$_2$ from a material surface by simply heating the material. In particular, porous materials functionalized with amines are under the spotlight due to their high adsorption capacity and simple synthetic procedure (wet impregnation) [8–11]. Among amines reported so far, polyethylenimine (PEI) supported on mesoporous support is advantageous over amines with low molecular weight, such as diethylenetriamine and tetraethylenepentamine, because PEI is more thermally stable and tolerant to oxidative conditions [12–14]. Its unique characteristic of enhanced CO$_2$ adsorption in the presence of moisture is also attractive for industrial applications. Branched PEI (BPEI) contains primary, secondary, and tertiary amines, and their CO$_2$ adsorption property is in the order of primary > secondary > tertiary [15]. Tertiary amines of BPEI do not adsorb CO$_2$

under dry conditions. So far, its application has been limited to CO_2 removal in spacecraft by NASA [16]. Large-scale industrial applications of BPEI for CO_2 capture demand significant improvements in the regeneration process in terms of energy consumption and long-term durability. CO_2 desorption from BPEI requires a relatively high temperature (>90 °C) [15]. Lowering the regeneration temperature contributes to a considerable decrease in the energy input and the total cost of capturing systems when long-term operation is considered without exchanging adsorbent materials for several years. In spite of its importance, lowering the regeneration temperature has not been the main focus in this field. One way to enhance CO_2 desorption was reported by using co-functionalization of BPEI with 1,2-epoxybutane [14]. The impregnation of BPEI onto a resin can also lower the desorption temperature down to 70 °C [17]. Previously, we also reported a reduction in the desorption temperature (50 °C) by co-impregnating BPEI with ionic liquids [6]. However, high toxicity and poor biodegradability of ionic liquids make their use in the environment unattractive [18]. PEI has another structure, which is linear PEI (LPEI). The utilization of LPEI for CO_2 capture was also extensively studied [19–27]. The adsorption capacity of LPEI is slightly low compared to BPEI, but LPEI has much better tolerance against oxidative conditions [24]. Similar to BPEI, LPEI also has a better adsorption capacity under humid conditions [25]. These properties make LPEI attractive for practical use. All the reports on LPEI focused on adsorption capacity, and its desorption property has never been a main target. In light of this, we focused on desorption properties of BPEI and LPEI in this study.

Among the three different amines of BPEI, primary amines are the most nucleophilic, with the highest pKa value [28,29]. Therefore, LPEI with high content of secondary amines would allow CO_2 desorption at a lower temperature. We herein report a comparative study of BPEI and LPEI, with a particular focus on CO_2 desorption properties.

2. Materials and Methods

2.1. Materials

Branched polyethylenimine (BPEI, Sigma-Aldrich, St. Louis, MO, USA; average Mw: ~25,000, average Mn: ~10,000), linear polyethlenimine (LPEI, Polysciences Inc., Warrington, PA, USA; average Mw: 250,000), silica (Sigma-Aldrich, St. Louis, MO, USA, fumed powder, average particle size: 0.2–0.3 μm), and ethanol (Acros Organics, Pittsburgh, PA, USA, 99.8%, anhydrous) were used as received without any purification. Helium (PanGas, Winterthur, Switzerland, ≥99.9999%) and 5000 ppm CO_2 in He balance (PanGas, Winterthur, Switzerland, ≥99.995% CO_2, ≥99.9999% He) were also utilized without any further purification.

2.2. Synthesis

PEI/SiO$_2$ adsorbents were prepared by a conventional wet-impregnation method as previously reported [6]. BPEI or LPEI was dissolved in anhydrous ethanol and stirred with a magnetic stirrer (IKA, Staufen, Germany, RCT standard) at room temperature for 30 min. The solution was then poured into a flask containing silica powders. The resulting suspension was vigorously stirred at room temperature for 1 h. The suspension was then transferred to a rotary evaporator (Büchi, Flawil, Switzerland, Rotavapor R-210) and slowly evacuated at 80 mbar and 32 °C to remove the ethanol solvent for 1 h. To completely dry the sample, it was kept under vacuum at 25–30 mbar at 50 °C for 20 min.

2.3. Adsorption and Desorption

The experimental set-up and procedure were exactly the same as in the previous report [6]. Briefly, CO_2 adsorption was performed in a fixed-bed plug-flow reactor. The CO_2 breakthrough was monitored by FT-IR spectrometer (Bruker, Billerica, MA, USA, ALPHA) equipped with a transmission gas-analysis module and deuterated triglycine sulfate (Bruker, Billerica, MA, USA, DTGS) detector. The adsorbent samples (300 mg) were placed into the tubular reactor and pretreated with a pure helium flow (200 mL/min) at 100 °C for 10 min (ramping rate: 5 °C/min). After pretreatment, the reactor was cooled

down to 25 °C, and the gas flow was switched to 5000 ppm CO_2 in He balance. Temperature-programmed desorption (TPD) was carried out by heating the reactor from 25 °C to 100 °C in a He flow at a ramping rate of 5 °C/min. Experiments under a humid condition were operated with a relative humidity (RH) of 73.9% (dew point: 20 °C). The details of the modulation excitation spectroscopy (MES) and diffuse reflectance infrared Fourier transform spectroscopy (ST Japan, Tokyo, Japan, DRIFTS) can be found in the previous report [6].

3. Results and Discussion

Figure 1a displays the molecular structures of BPEI and LPEI. BPEI consists of primary amines at branch ends, and secondary and tertiary amines in the backbone. In contrast, LPEI only contains secondary amines in the repetitive moiety. Both structures have one nitrogen atom in every three atoms in their backbone. Figure 1b shows a comparative study of CO_2 adsorption on 30 wt % BPEI/SiO_2 and 30 wt % LPEI/SiO_2 under dry and humid conditions. As commonly known [17], in the humid condition, CO_2 adsorption capacity increased by a factor of ca. 1.8 for both BPEI and LPEI (see Table 1). The presence of moisture accelerates the formation of bicarbonate species, and thus contributes to the increase in the adsorption capacity [17,25,30–32]. An important characteristic in the adsorption profile is that BPEI slowly adsorbed more CO_2 after reaching the CO_2 breakthrough point, most likely due to gas diffusion barriers in the highly viscous liquid BPEI layers on SiO_2 support (Figure 1b, red lines). On the other hand, LPEI is a solid polymer, and the gas diffusion in the solid phase is faster compared to a liquid layer. After saturating the materials with CO_2, temperature-programmed desorption (TPD) was carried out as shown in Figure 1c. As expected, the TPD peak top for LPEI (50.8 °C) dropped by ca. 30 °C, compared to BPEI (78.0 °C). As rationalized earlier by the nucleophilicity and pKa values [28,29], LPEI with a high concentration of secondary amine tremendously lowered the regeneration temperature. Both BPEI and LPEI adsorbed more CO_2 at 45 °C, as reported by the literature [26]. Previously, we reported lowering the regeneration temperature of BPEI by ionic liquid (IL) down to 50 °C [6]. However, BPEI-IL composite, in return, deteriorates the CO_2 adsorption property. LPEI can overcome this disadvantage by capturing relatively high amounts of CO_2 (Table 1). For example, LPEI showed high capturing performance (76.8 mg/g) at 45 °C. TPD could not be measured at 45 °C for LPEI, since all the CO_2 was released by switching to He. LPEI also desorbed CO_2 from the surface very slowly at 25 °C, which can be seen in Figure 1c. Hence, the interaction of CO_2 and secondary amines of LPEI was considered to be fairly weak. The N atom efficiency in Table 1 was estimated based on how many N atoms were actually used to capture CO_2. The maximum efficiency (41.5%) was achieved with 30 wt % BPEI/SiO_2 at 45 °C under a humid condition. At 25 °C, the N atom efficiency was nearly the same for both BPEI and LPEI under dry and humid conditions.

To evaluate the gas diffusion property, samples bearing 60 wt % PEI were also tested. As in Figure 2a and Table 1, 60 wt % BPEI adsorbed only 90.6 mg/g of CO_2, while 60 wt % LPEI captured 142.1 mg/g of CO_2. The increase in the loading amount had almost no positive effect for BPEI. As shown in Table 1, the N atom efficiency even dropped from 25.3% to 14.8% at 25 °C. This data implied that 30 wt % BPEI covered the entire surface of SiO_2, and further addition formed liquid overlayers, as schematically illustrated in Figure 2c. The high viscosity of liquid BPEI might make CO_2 diffusion inside the liquid layer difficult. Most likely, only the surface layer was accessible for CO_2 capture. This accounted for the reason for the low N atom efficiency for 60 wt % BPEI. However, LPEI with a melting point of 73–75 °C still seemed to have a permeable solid layer on SiO_2, and therefore, all the secondary amines were accessible for CO_2 adsorption. The N atom efficiency for LPEI was not influenced by the loading amount, as seen in Table 1. As shown in Figure 2b, TPD peak tops for both BPEI and LPEI shifted toward higher temperatures due to the diffusive barriers by loading 60 wt %.
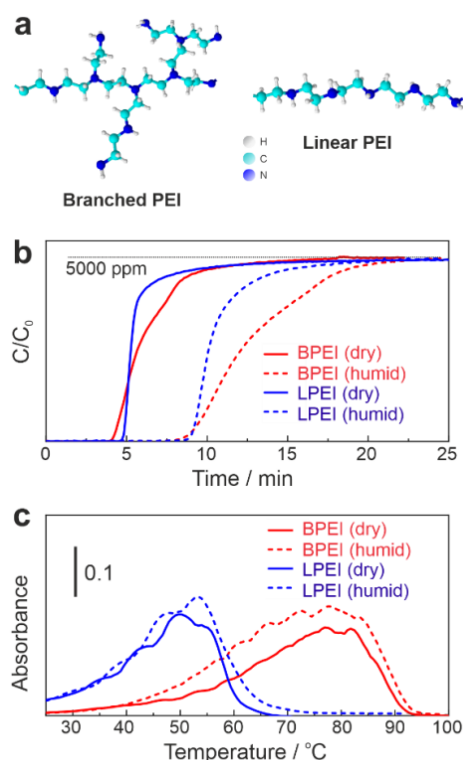
Figure 1. (**a**) BPEI and LPEI molecular structures; (**b**) CO_2 capture (5000 ppm CO_2 in He balance with/without H_2O vapor, 200 mL/min) at 25 °C; (**c**) TPD profile (5 °C/min, 200 mL/min of pure He).

Table 1. Adsorption and desorption performance of BPEI and LPEI supported on SiO_2 under different conditions. Note: 5000 ppm of CO_2 in He balance for adsorption and pure He for desorption. RH = 73.9% (dew point: 20 °C).
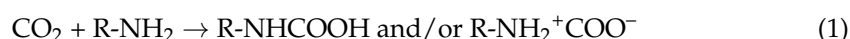
Adsorbent	Condition	Adsorption Capacity (mg/g) [#1]	N Atom Efficiency (%) [#4]	Desorption Temperature (°C) [#2]
30 wt % BPEI/SiO_2	25 °C, dry	41.2	13.5	78.0
30 wt % BPEI/SiO_2	25 °C, humid	77.5	25.3	78.6
30 wt % BPEI/SiO_2	45 °C, humid	127.0	41.5	67.1
60 wt % BPEI/SiO_2	25 °C, humid	90.6	14.8	96.7
30 wt % LPEI/SiO_2	25 °C, dry	37.6	12.3	50.8
30 wt % LPEI/SiO_2	25 °C, humid	68.6	22.4	54.4
30 wt % LPEI/SiO_2	45 °C, humid	76.8	25.1	_ [#3]
60 wt % LPEI/SiO_2	25 °C, humid	142.1	23.2	73.0

[#1] Amount of CO_2 captured (mg) per adsorbent used (g); [#2] peak centers of TPD profiles; [#3] all the CO_2 molecules were desorbed at 45 °C; [#4] the N atom efficiency was estimated based on the total number of N atoms in the samples. The maximum adsorption capacities were 306.3 mg/g for 30 wt % BPEI and LPEI and 612.7 mg/g for 60 wt % BPEI and LPEI.

To understand adsorption–desorption mechanisms at the molecular level, we applied in situ diffuse reflectance Fourier transform infrared spectroscopy (DRIFTS) combined with modulation excitation spectroscopy (MES) [33–35]. In situ MES-DRIFTS enhances the signal-to-noise (S/N) ratio, and thus allows in situ monitoring of a trace amount of active species involved in chemical reactions [33]. Figure 3a,b display time-domain IR spectra of BPEI and LPEI during repeated adsorption-desorption cycles at 50 °C. The spectral characteristics between BPEI and LPEI differed considerably; the absorbance for LPEI was higher by a factor of 10. This enhanced adsorption–desorption during modulation

experiment accounted for the lowered desorption temperature, releasing all the CO_2 at 50 °C within 200 s in the He flow. The IR bands observed for BPEI were well comparable to the ones previously reported [6]: ν(N-H) of carbamate and ammonium ion centered at around 3400 cm^{-1}, ν(C = O) of carbamic acid at 1680 cm^{-1}, ν(COO$^-$) of carbamate at 1558 cm^{-1}, δ(NH$_3^+$) of ammonium ion at 1530 cm^{-1}, and overlapped δ(N-H) and ν(C-N) of carbamate at 1502 cm^{-1}. As shown in Figure 3b, LPEI showed a completely different spectral feature. There were no IR bands assignable to carbamate or carbamic acid detected. Interestingly, ν(N-H) at around 3400 cm^{-1} completely disappeared. The band at 1405 cm^{-1} can also be assigned to ν(C-N). CO_2 adsorption with primary and secondary amines is considered to occur as follows [5]:

(Primary amines)

$$CO_2 + R\text{-}NH_2 \rightarrow R\text{-}NHCOOH \text{ and/or } R\text{-}NH_2{}^+COO^- \tag{1}$$

$$CO_2 + 2\,R\text{-}NH_2 \rightarrow R\text{-}NH_3{}^+ + R\text{-}NHCOO^- \tag{2}$$

(Secondary amines)

$$CO_2 + 2R1(R2)\text{-}NH \rightarrow R1(R2)\text{-}NCOO^- + R1(R2)\text{-}NH_2{}^+ \tag{3}$$

Reaction (1) forms carbamic acid or carbamate ion involving one amine group. Reactions (2) and (3) involve two amine groups. The spectral analysis based on Figure 3 led us to come to an assumption with the following reaction path:
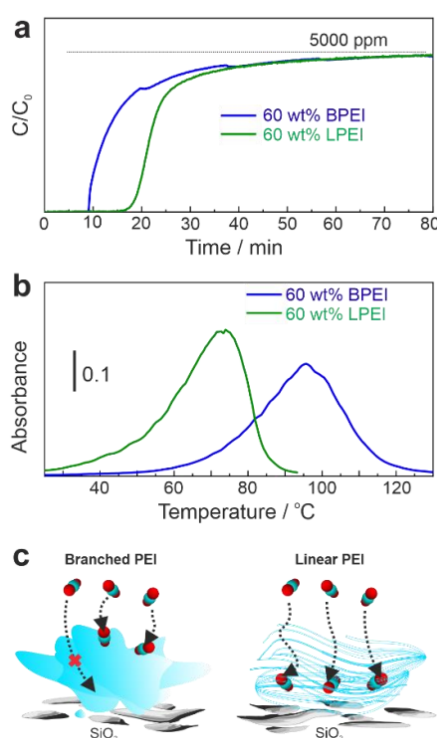
$$CO_2 + R1(R2)\text{-}NH \rightarrow R1(R2)\text{-}NCOOH \tag{4}$$

Figure 2. Effect of loading amount of PEI on (**a**) CO_2 capture and (**b**) desorption (conditions are identical to the experiments in Figure 1 with H_2O). (**c**) Schematic illustration of CO_2 diffusion.

This model would fit to our spectral observation. This assumption was further supported by the detection of the broad band of ν(O-H) at 3000–3200 cm^{-1}. To the best of our knowledge, there has been no previous report proposing such an adsorption configuration

together with spectroscopic evidence. This configuration provides a rational basis for future molecular design of CO_2 adsorbents for low-temperature regeneration.
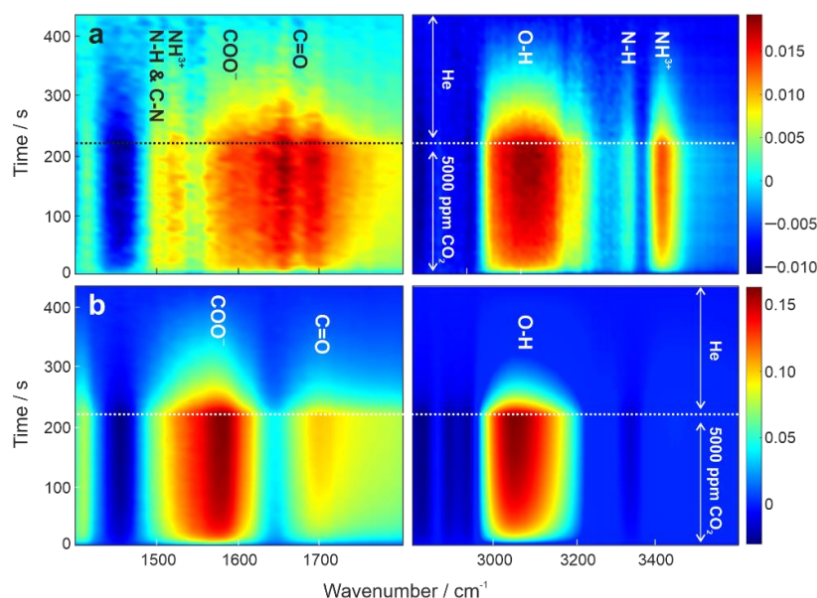

Figure 3. Time-domain IR contour plots of (**a**) 30 wt % BPEI/SiO_2 and (**b**) 30 wt % LPEI/SiO_2 during CO_2 adsorption–desorption at 50 °C (5000 ppm CO_2 in He balance: 200 mL/min, pure He: 200 mL/min). The unit of the color bar is absorbance.

Finally, we tested 30 wt % LPEI/SiO_2 for recyclability. The adsorption–desorption cycles at 45 °C under humid conditions were repeated; 5000 ppm CO_2 in He balance with H_2O vapor at 200 mL/min was fed into the reactor and then switched to pure He for desorption cycles (Supplementary Materials). As seen in Figure 4, within 100 cycles there was no performance deterioration observed. LPEI could release all the CO_2 molecules at 45 °C, and therefore has a high potential for industrial applications.
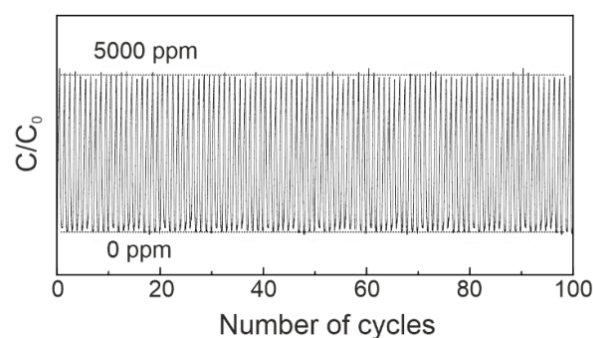

Figure 4. The recyclability test for adsorption and desorption of CO_2 at 45 °C (50 mg, 5000 ppm CO_2 in He balance: 200 mL/min, pure He: 200 mL/min).

4. Conclusions

We compared BPEI and LPEI supported on SiO_2, aiming at low-temperature regeneration. We found that 30 wt % LPEI/SiO_2 could be regenerated below 50 °C. This unique property originated from different adsorption configurations of CO_2 between BPEI and LPEI. MES-DRIFTS analysis proved that CO_2 adsorption on BPEI fell into the classical adsorption model involving carbamic acid, carbamate, and ammonium ions. On the other hand, such a model could not be applied for interpreting the CO_2 adsorption on LPEI.

Based on the in situ IR spectral analysis, we propose the intermediate species to be R1(R2)-NCOOH, which can be decomposed at 25–50 °C to release CO_2. The newly proposed model will pave the way for rational molecular design of amine-based polymers targeting low-temperature regeneration in CO_2 capture.

References

1. Cui, Y.; Schubert, B.A.; Jahren, A.H. A 23 m.y. record of low atmospheric CO_2. *Geology* **2020**, *48*, 888–892. [CrossRef]
2. Wilson, S.M.W.; Tezel, F.H. Direct Dry Air Capture of CO_2 Using VTSA with Faujasite Zeolites. *Ind. Eng. Chem. Res.* **2020**, *59*, 8783–8794. [CrossRef]
3. Yoro, K.O.; Daramola, M.O.; Sekoai, P.T.; Armah, E.K.; Wilson, U.N. Advances and emerging techniques for energy recovery during absorptive CO_2 capture: A review of process and non-process integration-based strategies. *Renew. Sustain. Energy Rev.* **2021**, *147*, 111241. [CrossRef]
4. Bains, P.; Psarras, P.; Wilcox, J. CO_2 capture from the industry sector. *Prog. Energy Combust. Sci.* **2017**, *63*, 146–172. [CrossRef]
5. Heldebrant, D.J.; Koech, P.K.; Glezakou, V.-A.; Rousseau, R.; Malhotra, D.; Cantu, D.C. Water-Lean Solvents for Post-Combustion CO_2 Capture: Fundamentals, Uncertainties, Opportunities, and Outlook. *Chem. Rev.* **2017**, *117*, 9594–9624. [CrossRef]
6. Weisshar, F.; Gau, A.; Hack, J.; Maeda, N.; Meier, D.M. Toward Carbon Dioxide Capture from the Atmosphere: Lowering the Regeneration Temperature of Polyethylenimine-Based Adsorbents by Ionic Liquid. *Energy Fuels* **2021**, *35*, 9059–9062. [CrossRef]
7. Rochelle, G.T. Amine Scrubbing for CO_2 Capture. *Science* **2009**, *325*, 1652. [CrossRef]
8. D'Alessandro, D.M.; Smit, B.; Long, J.R. Carbon Dioxide Capture: Prospects for New Materials. *Angew. Chem. Int. Ed.* **2010**, *49*, 6058–6082. [CrossRef]
9. Hedin, N.; Bacsik, Z. Perspectives on the adsorption of CO_2 on amine-modified silica studied by infrared spectroscopy. *Curr. Opin. Green Sustain. Chem.* **2019**, *16*, 13–19. [CrossRef]
10. Kuang, Y.; He, H.; Chen, S.; Wu, J.; Liu, F. Adsorption behavior of CO_2 on amine-functionalized polyacrylonitrile fiber. *Adsorption* **2019**, *25*, 693–701. [CrossRef]
11. Tanthana, J.; Chuang, S.S.C. In Situ Infrared Study of the Role of PEG in Stabilizing Silica-Supported Amines for CO_2 Capture. *ChemSusChem* **2010**, *3*, 957–964. [CrossRef]
12. Liu, Z.L.; Teng, Y.; Zhang, K.; Chen, H.G.; Yang, Y.P. CO_2 adsorption performance of different amine-based siliceous MCM-41 materials. *J. Energy Chem.* **2015**, *24*, 322–330. [CrossRef]
13. Olea, A.; Sanz-Perez, E.S.; Arencibia, A.; Sanz, R.; Calleja, G. Amino-functionalized pore-expanded SBA-15 for CO_2 adsorption. *Adsorption* **2013**, *19*, 589–600. [CrossRef]
14. Choi, W.; Min, K.; Kim, C.; Ko, Y.S.; Jeon, J.W.; Seo, H.; Park, Y.-K.; Choi, M. Epoxide-functionalization of polyethyleneimine for synthesis of stable carbon dioxide adsorbent in temperature swing adsorption. *Nat. Commun.* **2016**, *7*, 12640. [CrossRef]
15. Wang, X.; Song, C. Temperature-programmed desorption of CO_2 from polyethylenimine-loaded SBA-15 as molecular basket sorbents. *Catal. Today* **2012**, *194*, 44–52. [CrossRef]
16. Satyapal, S.; Filburn, T.; Trela, J.; Strange, J. Performance and properties of a solid amine sorbent for carbon dioxide removal in space life support applications. *Energy Fuels* **2001**, *15*, 250–255. [CrossRef]
17. Wang, W.; Liu, F.; Zhang, Q.; Yu, G.; Deng, S. Efficient removal of CO_2 from indoor air using a polyethyleneimine-impregnated resin and its low-temperature regeneration. *Chem. Eng. J.* **2020**, *399*, 125734. [CrossRef]
18. Thi, P.T.P.; Cho, C.W.; Yun, Y.S. Environmental fate and toxicity of ionic liquids: A review. *Water Res.* **2010**, *44*, 352–372. [CrossRef]
19. Buijs, W. Molecular Modeling Study to the Relation between Structure of LPEI, Including Water-Induced Phase Transitions and CO2 Capturing Reactions. *Ind. Eng. Chem. Res.* **2021**, *60*, 11309–11316. [CrossRef]
20. Prud'homme, A.; Nabki, F. Comparison between Linear and Branched Polyethylenimine and Reduced Graphene Oxide Coatings as a Capture Layer for Micro Resonant CO_2 Gas Concentration Sensors. *Sensors* **2020**, *20*, 1824. [CrossRef]

21. Rosu, C.; Pang, S.H.; Sujan, A.R.; Sakwa-Novak, M.A.; Ping, E.W.; Jones, C.W. Effect of Extended Aging and Oxidation on Linear Poly(propylenimine)-Mesoporous Silica Composites for CO_2 Capture from Simulated Air and Flue Gas Streams. *ACS Appl. Mater. Interfaces* **2020**, *12*, 38085–38097. [CrossRef] [PubMed]

22. Sharma, P.; Chakrabarty, S.; Roy, S.; Kumar, R. Molecular View of CO_2 Capture by Polyethylenimine: Role of Structural and Dynamical Heterogeneity. *Langmuir* **2018**, *34*, 5138–5148. [CrossRef] [PubMed]

23. Subagyono, D.J.N.; Marshall, M.; Knowles, G.P.; Chaffee, A.L. CO_2 adsorption by amine modified siliceous mesostructured cellular foam (MCF) in humidified gas. *Microporous Mesoporous Mater.* **2014**, *186*, 84–93. [CrossRef]

24. Yoo, C.-J.; Park, S.J.; Jones, C.W. CO_2 Adsorption and Oxidative Degradation of Silica-Supported Branched and Linear Aminosilanes. *Ind. Eng. Chem. Res.* **2020**, *59*, 7061–7071. [CrossRef]

25. Zhang, H.; Goeppert, A.; Olah, G.A.; Prakash, G.K.S. Remarkable effect of moisture on the CO2 adsorption of nano-silica supported linear and branched polyethylenimine. *J. CO2 Util.* **2017**, *19*, 91–99. [CrossRef]

26. Zhang, H.; Goeppert, A.; Prakash, G.K.S.; Olah, G. Applicability of linear polyethylenimine supported on nano-silica for the adsorption of CO_2 from various sources including dry air. *RSC Adv.* **2015**, *5*, 52550–52562. [CrossRef]

27. Zhou, Z.; Balijepalli, S.K.; Nguyen-Sorenson, A.H.T.; Anderson, C.M.; Park, J.L.; Stowers, K.J. Steam-Stable Covalently Bonded Polyethylenimine Modified Multiwall Carbon Nanotubes for Carbon Dioxide Capture. *Energy Fuels* **2018**, *32*, 11701–11709. [CrossRef]

28. Suh, J.; Paik, H.J.; Hwang, B.K. Ionization of Poly(ethylenimine) and Poly(allylamine) at Various pH's. *Bioorg. Chem.* **1994**, *22*, 318–327. [CrossRef]

29. Sun, C.; Tang, T.; Uludağ, H.; Cuervo, J.E. Molecular Dynamics Simulations of DNA/PEI Complexes: Effect of PEI Branching and Protonation State. *Biophys. J.* **2011**, *100*, 2754–2763. [CrossRef]

30. Li, K.J.; Kress, J.D.; Mebane, D.S. The Mechanism of CO_2 Adsorption under Dry and Humid Conditions in Mesoporous Silica-Supported Amine Sorbents. *J. Phys. Chem. C* **2016**, *120*, 23683–23691. [CrossRef]

31. Sayari, A.; Belmabkhout, Y. Stabilization of Amine-Containing CO_2 Adsorbents: Dramatic Effect of Water Vapor. *J. Am. Chem. Soc.* **2010**, *132*, 6312–6314. [CrossRef]

32. Veneman, R.; Frigka, N.; Zhao, W.Y.; Li, Z.S.; Kersten, S.; Brilman, W. Adsorption of H_2O and CO_2 on supported amine sorbents. *Int. J. Greenh. Gas Control.* **2015**, *41*, 268–275. [CrossRef]

33. Maeda, N.; Meemken, F.; Hungerbuhler, K.; Baiker, A. Spectroscopic Detection of Active Species on Catalytic Surfaces: Steady-State versus Transient Method. *Chimia* **2012**, *66*, 664–667. [CrossRef]

34. Muller, P.; Hermans, L. Applications of Modulation Excitation Spectroscopy in Heterogeneous Catalysis. *Ind. Eng. Chem. Res.* **2017**, *56*, 1123–1136. [CrossRef]

35. Urakawa, A.; Burgi, T.; Baiker, A. Sensitivity enhancement and dynamic behavior analysis by modulation excitation spectroscopy: Principle and application in heterogeneous catalysis. *Chem. Eng. J.* **2008**, *63*, 4902–4909. [CrossRef]